Trends and Variability in Summer Precipitation and Streamflow in the upper Gila River basin

David S. Gutzler, Ph.D.

Submitted to the New Mexico Interstate Stream Commission

Deliverable 1

Contract Number PSA 19179

November 2, 2015

revised June 3, 2016

Contents

1. Introduction

This paper discusses variability and trends of warm season precipitation and streamflow in the upper Gila River basin, southwestern New Mexico. The early months of the summer is the low flow season in the upper Gila (Gutzler 2013; Horner and Dahm 2014; Garfin et al. 2014). Flows reach a minimum after snowmelt runoff occurs in late winter and spring, and before the summer monsoon season has recharged the basin with intermittent, high intensity rainfall events (Gutzler 2013). Low flows limit ecological productivity in and around the Gila River, and therefore also place limits on potential water withdrawals from the river. The papers cited above were prepared for the purpose of providing guidance on projected future flows in the Gila River, for use regarding decisions on water allocations and potential diversions within New Mexico related to the 2004 Arizona Water Settlements Act.

This paper describes low flows, and the precipitation during the low flow season, as the initial phase of a contract from the New Mexico Interstate Stream Commission with the objective of characterizing observed and projected precipitation and flows during the low flow season on the upper Gila River. The objective of this paper is to "provide a comparative analysis of warm season flows and precipitation in the historical observed record and in climate model projections." The hydroclimatic mechanisms responsible for limiting and modulating precipitation and flow during the low flow season will be examined in the subsequent analysis phase of this contract. Thus this paper, constituting Deliverable 1, will provide the observational foundation for forthcoming research supported by funding from this contract.

Garfin et al. (2014) and Gutzler (2013) identified the summer season as a period when uncertainty in precipitation, and therefore streamflow, is large. In observations, summer convective thunderstorms tend to be small in scale, so individual storms do not cover the upper Gila watershed and precipitation measurements are difficult. In models, summer convective thunderstorms are challenging to simulate, and differences in model projections of future convective precipitation are large (Garfin et al. 2014).

Following the general analysis procedure used by Gutzler (2013), the present study is based on both observed data for both streamflow and precipitation and model-based

future projections of these variables. For observed streamflow, the analysis uses daily discharge estimated at the USGS gage near Gila on the upper Gila River (USGS gage number 09430500; Fig. 1). Data from this gage, hereafter referred to as the "Gila gage", was heavily used by analysts contributing to the Nature Conservancy's volume of papers describing multiple studies of upper Gila River hydrology and ecology (Gori et al. 2014), including the papers on Gila flow projections by Horner and Dahm (2014) and Garfin et al. (2014).

For precipitation, the present analysis uses time series of observed monthly precipitation estimated for the spatial area corresponding to the watershed upstream of the Gila gage by the Westmap project, obtained from the Western Regional Climate Center in Reno NV. The Westmap precipitation product, derived from high-resolution spatial analysis of raingage data using the well-established PRISM interpolation algorithm (Daly et al. 2008), is different from the Climate Divisional spatial average of precipitation used by Gutzler (2013), and should correspond more closely to precipitation actually affecting the flow at the Gila gage. Although the Divisional spatial average proved to be well-correlated with Gila gage flows for the snowmelt runoff season, the patchy nature of summer convective precipitation makes the use of broad-scale summer Climate Divisional values problematic (Pascolini-Campbell et al. 2015) so we use the Westmap average in this analysis.

There are some differences in the observed data sets for precipitation and streamflow that affect interpretation of the analysis that follows. The Westmap precipitation data are available through 2014, whereas we had access to gage data through the summer of 2015. The most recent streamflow data are retained in the analysis, but correlative comparisons between observed precipitation and streamflow extend only through 2014.

Trends and variability of observed flows and precipitation are compared with corresponding model-simulated values generated by the U.S. Bureau of Reclamation as part of their WestWide Climate Assessment project (Reclamation 2011a,b). The present study uses output from the same 39 global climate model simulations examined by Gutzler (2013). These simulation start in 1950 and use historical greenhouse gas forcing until the early 21st Century; all simulations are then forced in future years by the same scenario (denoted A1B) of increasing Greenhouse Gas concentrations (Meehl et al. 2007). The A1B scenario has generally been considered to be a midrange estimate of greenhouse gas

forcing through the 21st Century. For this study we will consider future projection through year 2050; previous studies have determined that the choice of greenhouse gas forcing scenario does not dramatically affect climate change trajectories until later in the 21st Century (IPCC 2007, 2013; Gutzler and Robbins 2011).

The output from each coarse-resolution global climate model was downscaled across the western United States as part of BoR's WestWide Assessment (BoR 2011b). Downscaled surface variables from the model output were used to drive a surface hydrologic model, the Variable Infiltration Capacity (VIC) model (Liang et al. 1994). VIC simulates surface flows using runoff that flows downstream routed by a digital elevation model. For this study no additional downscaling or bias correction has been implemented; we have used BoR's output which is available online. Subsequent to the original WestWide Assessment (BoR 2011a), which used global climate simulations generated as part of the CMIP3 coordinated set of model runs (Meehl et al. 2007), a new set of global model runs, known as CMIP5 (Taylor et al. 2012) was generated in support of the 2013 IPCC change assessment. BoR has augmented their CMIP3-based hydrology projections with a new set of projections based on the CMIP5 models. However for this study we have chosen to stick with the older CMIP3-based output, to remain consistent with previous assessments of Gila River flows carried out as part of AWSA planning efforts (Gutzler 2013; Garfin et al. 2014).

We will consider flows draining the upper Gila basin at a pour point in BoR's digital elevation model corresponding to the location of the Gila gage. Given all the multiple uncertainties in modeling -- in the forcing functions that drive the global climate models, in the processes simulated by those climate models, in the downscaling to higher resolution, in the coupling to the hydrologic model, and in the hydrologic model itself -- we do not expect the simulated Gila gage flows to exactly match the observations, but we do expect high-quality simulations to reproduce the statistics of hydroclimatic trends and variability representative of observed flows. For each model, BoR has provided access to simulated precipitation in the upper Gila basin upstream from the designated pour point. Therefore the simulated and observed precipitation values are calculated over the same spatial averaging region, so the statistics of simulated and observed precipitation should be directly comparable.

The model simulations are initialized using prescribed climate forcing and initial conditions appropriate for the middle of the 20th Century. Output is available starting in simulated year 1951, and continues through the 21st Century. As stated above, this study will consider the observed record of precipitation and streamflow for the period 1930-2015, and will compare those results simulated precipitation and streamflow for the period 1951-2050 from BoR (2011a, b). The use of 39 identically-forced simulations allows the analysis to explore uncertainty associated with model-to-model differences in response to the same forcing.

The Westmap precipitation data are available only as monthly averaged values, and the projected precipitation and streamflow values are also available as monthly values. Therefore most of this analysis will be based on monthly values of precipitation and streamflow, either observed or simulated. Monthly averages of these hydroclimatic variables are appropriate for a climatic analysis. However the availability of daily stream-flow observations will allow us to confirm that observed changes in the statistics of monthly and daily low-flow season streamflow are comparable.

General assessments of historical streamflow variability in the upper Gila basin, and the precipitation and temperature fluctuations modulating streamflow variability, were described by Gutzler (2013) and Garfin et al. (2014) as part of previous AWSA planning activities. A subsequent paper by Pascolini-Campbell et al. (2015) extended the results to examine more explicitly the large-scale climate variability that leads to local precipitation and snowpack fluctuations in the upper Gila basin. A very large fraction of the analysis in the these existing assessments focused on the high-flow part of the seasonal hydrograph during the late winter and spring seasons. A considerable fraction of the interannual variance of historical observations can be attributed to large-scale shifts in cold season storm tracks, which in turn are highly correlated with Pacific Ocean temperature. As climate warms, future snow-fed streamflow is projected to be diminished by the reduction in snowpack resulting from significantly warmer temperature.

In this paper we focus specifically on low flow months of June and July at the Gila gage. Examination of the historical record clearly identifies June and July as the low-flow months at the Gila gage (Fig. 2, reproduced from Gutzler 2013). The climatological processes that determine streamflow are considerably different in these warm season months compared

to the processes that predominate in the high-flow snowmelt runoff season (Tuan et al. 1972; Garfin et al. 2014). Precipitation in the warm season is largely convective in nature, delivered from relatively small-scale but intense thunderstorms, instead of the broad frontal systems that bring precipitation in the cold season. Although warm season thunderstorms are sufficiently organized to form an identifiable monsoon season (Hales 1972; Douglas et al. 1993; Higgins et al. 1997), model simulation and prediction of thunderstorm activity is relatively uncertain compared to winter precipitation. On longer time scales, interannual variability of winter precipitation is much better defined and predictable than is precipitation in the warm season. The El Niño-Southern Oscillation (ENSO) cycle accounts for a significant fraction of winter and early spring interannual variability across Southwestern North America (Ropelewski and Halpert 1986; Redmond and Koch 1991) but ENSO provides much less predictability in the warm season months (Gutzler and Preston 1993). Some of the largest precipitation and streamflow events in the Southwest occur as the result of warm season tropical cyclone remnants (Etheredge et al. 2004; Ritchie et al. 2011), and these storms are very difficult to predict. The CMIP3 coupled climate models do include thunderstorms, tropical cyclones, and ENSO variability, although the model-to-model differences in simulating these phenomena are very considerable (IPCC 2007; Jones and Gutzler 2016). The challenges inherent in large-scale modeling of warm season climate add to the general uncertainty of predicting future streamflow in the upper Gila basin.

The months of June and July are selected for more in-depth analysis in terms of observations (Section 2 of this paper) and climate model simulations and projections (Section 3). Interpretive comments on the results, and a discussion of uncertainties and limitations of the analysis, are presented in Section 4. A summary of principal conclusions is given in Section 5.

2. Observed Summer Trends and Variability of Streamflow and Precipitation in the Upper Gila Basin

The historical record of monthly precipitation in June, from 1930 to 2014, contains no statistically significant trend over the entire period of record based on a linear fit to the time series (not shown). As shown in Fig. 3, the year-to-year variability of June precipi-

tation is very large compared to the climatological average value of precipitation. The median monthly precipitation rate for the entire record is 0.37 mm/d (equivalent to total monthly precipitation of 0.44 inches), but values about the long-term average range from a minimum monthly rate 0.01 mm/d in 1951 to a maximum of 1.80 mm/d in 2000.

One way to try to separate long-term change from shorter term interannual or decadal variability in the data is to consider the statistics of the first and second halves of the data, and check for differences in the distribution of precipitation between these samples. Box-and-whiskers plots (henceforth called "distribution plots") for observed June precipitation are shown in Fig. 3b, calculated separately for the periods 1930-1972 and 1973-2014, the first and second halves of the data record. The precipitation values corresponding to the 25th and 75th percentiles of the distributions form the box, with a horizontal line within each box marking the 50th percentile (the median value of monthly June precipitation). These same percentile values are shown on the time series plot in Fig. 3a as horizontal lines. The whiskers extend downward and upward from each box to the 5th and 95th percentiles, respectively, of each distribution. The whiskers therefore describe the distribution of extreme events, keeping in mind that one or two exceptional values exist outside the range of the whiskers. The presence of these rare exceptional values is represented in Fig. 3b by printing the maximum value in each half of the data record above the respective 95th percentile whisker.

In the observed June precipitation record, the 5% whisker is nearly zero in both halves of the record and changes little from the first to the second half of the record. The recent multi-year drought is exceptional, in that monthly precipitation in each of the final four years of the data record (2011-2014) lies below the 25th percentile. The 25th, 50th, and 75th percentile values all decrease slightly in the second half of the record (shown in both Fig. 3a and Fig. 3b), although the highest single extreme value occurs in the second half of the record in year 2000. The climatic changes in these percentile values are not statistically significant, and overall our assessment is that the statistics of June precipitation have not changed much over the historical period of record.

Time series and distribution plots for July precipitation, using the same plotting conventions already described for the June results, are shown in Figs. 4a and 4b. As was the case in June, the 5% threshold of extreme low values does not change significantly from the

first to the second half of the data record, and the 25% threshold decreases only slightly. Unlike the June precipitation results, the median, 75% and 95% values of precipitation increase significantly in July data. In other words, average and above-average precipitation values increase in the latter half of the observed record, while low precipitation values do not change much. Therefore the overall variability of precipitation increases significantly, driven by an increase in the high end of monthly precipitation values as shown by the 95th percentile and maximum values in Fig. 4b. The increase in high values of precipitation in recent years is clearly evident from visual inspection of Fig. 4a.

Figures 5 and 6 show time series and distribution plots for monthly streamflow values in the low-flow months of June and July, which can be compared to the precipitation plots just shown. The difference in the statistics of low flows between the first and second halves of the record in June (Fig. 5) is similar to the June precipitation statistics: a slight decrease in the 25% threshold, with a succession of very low values at the end of the data record during the recent drought. Note that data for 2015 were not available for precipitation, but are analyzed here for streamflow and are included in the statistics underpinning Fig. 5. Streamflow in June 2015 was somewhat higher compared to the previous four years. However the statistics of high-flow values in June shows a significant increase in variability. Low flows, represented by the 25% threshold, are lower, whereas the median flow is higher and extreme high flows are significantly higher.

Median and high flows have also increased in recent decades in July (Fig. 6), driven by the corresponding increase in median and high precipitation values in the second half of the record (Fig. 4). As above-average precipitation values increased in the late 20th Century during the start of the monsoon season in July, high-flow values of streamflows at the Gila gage also increased in July. Below-average flows show less evidence of change from the first to the second halves of the data record.

Assessment of precipitation and streamflow values during the low-flow months of June and July must consider these two months separately, because the relationship between precipitation and streamflow is quite different in these two months. Typically the monsoon season has not started in the month of June, as shown by the much lower average values of precipitation in June compared to July (Figs. 3, 4). Monthly precipitation in June is, in fact, not significantly correlated with concurrent streamflow: the linear correlation

coefficient between interannual fluctuations of precipitation and streamflow in the observed record is only 0.13. Flows in June are, instead, highly correlated with preceding streamflow in May: the autocorrelation in monthly flow anomalies from May to June is 0.92. Thus the flow at the Gila gage in June is dominantly affected by the snowmelt-driven flows of late Spring.

In contrast, July flows only weakly correlated with May or June flows: the auto-correlation of June flows with July flows is only 0.24. Instead, flows in July are high when the early monsoon is strong during the same month, and low when July precipitation is deficient: correlation between July precipitation and streamflow is 0.60, highly statistically significant. In summary, July flows, in the current climate and in future projections of climate, are strongly tied to monsoon precipitation, whereas June flows are more strongly modulated by the preceding winter's snowpack and subsequent snowmelt runoff.

The preceding assessment is based on monthly averages of precipitation and stream-flow, limited by the non-availability of daily precipitation spatially averaged over the upper Gila basin. However we can compare the statistics of observed monthly-averaged stream-flow to the statistics of daily streamflow values at the Gila gage. Distribution plots derived from daily values of flow in June and July (Fig. 7) can be compared with the distri-butions of monthly averages, derived from exactly the same data set, in Figs. 5b and 6b. In June, we find that extreme values of daily streamflow within the month are very highly correlated with monthly values and changes from the first to the second halves of the data record are very similar. The 10th percentile of daily flows within each June month (i.e. extreme low flows each year) and the 90th percentile of daily flows (extreme high flows for June each year) are both correlated better than 0.9 with interannual variability of monthly average flows. We conclude that June monthly averages are highly representative of extreme flows in June, so that trends in monthly averages can be interpreted in terms of trends in daily extreme flows with confidence.

In July, when flows are more tightly coupled to convective rainfall events associated with monsoon onset, these correlations are somewhat lower. Monthly average streamflow is correlated with 10th percentile daily low flows at a value of r=0.72; that is, about half of the interannual variance of extreme low flows is accounted for by interannual fluctuations of July monthly mean flow. The corresponding correlation between the monthly mean flow

and 90th percentile daily flow in July is 0.89, somewhat higher. This result indicates that the monthly mean streamflow in July is somewhat more indicative of higher flows than extreme low flows during the month. The same conclusion is derived from comparison of changes in the distribution plots for July streamflows based on monthly (Fig. 6b) and daily (Fig. 7b) data, which both show substantial increases in high flows (75th percentile and higher).

3. Projected Summer Trends and Variability of Streamflow and Precipitation in the Upper Gila Basin

In this section, simulated precipitation and streamflow for June and July from the Westwide hydrologic assessment (BoR 2011) are described. As outlined in the Introduction, we use simulations for the period 1951-2050. Our goals in this section are to (a) describe trends in precipitation and streamflow across this period of time, and changes in the distribution of June or July precipitation and streamflow from the first half (1951-2000) to the second half (2001-2050) of these simulations, and (b) to compare trends and distributions in the simulations to the observed changes documented in the previous section. Confidence in simulated changes is increased if we see analogous changes in observations from the first to the second half of the observational period of record, during a period of a significant warming trend in New Mexico. If similar changes between simulations and observations is found, then it is more justified to consider the simulated changes extending into the future (through 2050) as likely to occur.

As in observations, median June precipitation in the upper Gila basin averaged over 39 simulations exhibits no significant long-term trend (Fig. 8). Most of the distribution of monthly precipitation values also exhibits no significant difference between the first and second halves of the data record. However there is an increase in high-precipitation months, indicated by an increase in 75th percentile values (Fig. 8b) and in the extreme high-precipitation months beyond the 75th percentile. Similar results are found in July (Fig. 9): no overall trend in average precipitation rate, and no significant changes in low flows, but an increase in the extreme high flow months.

Despite the relatively stationary statistics of June precipitation, for which most of the distribution of monthly precipitation values shows no change over the century of simu-

lation, the corresponding June streamflows for the 95th percentile and below decrease significantly into the 21st Century (Fig. 10). Decreases in low flows, median flows, and high flows are clearly evident in the distribution plots for June streamflow simulations (Fig. 9b). However the most extreme monthly flows, above the 95th percentile, increase as seen in the increase in absolute maximum values.

The sharp increase in the very highest flows affects trend statistics for streamflow, and creates a significant difference in the statistics of mean vs median flows. A linear trend line fit to the time series of median June streamflow, averaged over all 39 simulations (the heavy solid line in Fig 9a), is -14 (mm/d) per century, representing a substantial decrease in low season flow in June, prior to the onset of monsoon precipitation.

July streamflow changes are somewhat different than the June results in the simulations. Median values show a very slight (statistically insignificant) decrease, but 75th percentile high flows show no change and extreme high flows (95th percentile) are considerably higher in the 2001-2050 period (Fig. 10b). These increases in streamflow correspond well with the simulated increases in July precipitation (Fig. 8), as would be expected given the high correlation between July precipitation and July streamflow in observations. Our analysis of daily observed streamflow indicates that the increase in high flow months in future years in the simulations can be interpreted as an increase in high extreme daily flows, indicative of an increase in the intensity of convective rainfall as the climate warms during the 21st Century.

The trend in July flow, averaged over all 39 simulations, is affected so strongly by the increase in above-average flows in the later years of the simulation period that trends based on means or medians have the opposite sign. The linear trend fit to 39-simulation averages of *median* flow (shown in Fig. 10b) is -8 cfs/century. However the trend in average *mean* flow, more strongly affected by individual extreme high-flow months, is upward: +5 cfs/century, i.e. July mean flow in the 39-member average increases as climate warms. Both of these trends are small in magnitude, and both represent a near-zero average of widely disparate model results (some models generate apparently significant increases, others generate large decreases). The number of simulations exhibiting negative or positive linear trends in July streamflow was split as evenly as possible (20 negative trends, 19 positive trends among the 39 simulations). In summary, trends in simulated July

streamflow are not significant, referring to monthly-average flows averaged over many model simulations; however, the high-flow end of the distribution of monthly flows increases in July across the ensemble of models.

4. Discussion

This analysis was motivated by large uncertainties in the low-flow season found in previous analyses of the hydroclimatic variability in the upper Gila basin. The analysis of precipitation and streamflows presented here, going into considerably more depth than the previous set of AWSA-associated assessments (Horner and Dahm 2014; Garfin et al. 2014; Gutzler 2013) serves to reiterate this uncertainty. In observations, trends are small compared to interannual variability, although the data suggest the presence of some shifts that are difficult to assess using formal significance tests. In particular, the magnitude of variability has increased in July precipitation, and in June and July streamflows. Even this result might conceivably be attributed to several decades of relatively wet climatic conditions in the late 20th Century followed by an exceptionally severe drought at the end of the data record (instead of associated the increase in variability to warmer temperatures).

Simulated streamflow and precipitation present clearer signals than observations. Although trends in average monthly precipitation are not consistently projected across the ensemble of models, high-end precipitation values tend to increase. In simulations, June streamflow decreases as climate warms despite uncertainties in precipitation projections.

Is the latter result one that should be trusted? There is a small, but statistically significant, decrease in observed average June streamflow values, broadly coincident with an warming trend in the observed data during the second half of the data record. It is possible that a temperature-driven decrease in June flow has been temporarily obscured by a natural, multidecadal pluvial period that ended several years ago, but this is difficult to prove based on the available data record.

In model simulations, at least part of a decrease in projected June flows is probably the result of a tendency for climate models to delay the start of the summer monsoon season as a response to rising late spring temperature (Cook and Seager 2013). But there is no definitive support for a systematic delay in monsoon onset in observations of recent

climate change (Gutzler and Keller 2011) so this mechanism for changing low season flows still remains questionable.

Any study involving climate model projections must acknowledge the uncertainties and limitations inherent in such models. Coupled models, such as the BoR's modeling system that couples downscaled global climate model output to a hydrologic model, are all prone to multiple sources of uncertainty, as was discussed in the Introduction. This study, unlike the Garfin et al. (2013) approach to multi-model assessment, has chosen not to attempt to discriminate "better" model simulations from "worse" simulations. Instead, like the BoR approach, we choose to rely on the statistics of large model ensembles to distinguish consistent signals from individual model outlier results.

With this difference in mind, we note that the results of this analysis concerning the consistent tendency for an increase in future decades in the magnitude of projected high-precipitation and high-flow events in July, is broadly consistent with results presented by Garfin et al. (2014). The agreement here is significant, because of the different modeling strategy employed by Garfin et al. (2014). The Garfin et al. study was based on a much smaller set of model simulations, in which dynamical downscaling was employed in an effort to improve the reliability of future precipitation estimates. They argued that high-resolution dynamical models should generate better estimates of small-scale convective rainfall (i.e. thunderstorms) than the statistical downscaling carried out in the BoR simulations. Gutzler (2014) reviewed the Garfin et al. study and argued that, even if some individual simulations seem deficient, BoR's downscaling approach might mitigate their effect via the statistical advantage inherent in using a large ensemble of models, as mentioned above. Regardless of which approach to coupling coarse resolution climate models to higher resolution hydrologic models is best, the general agreement found here in the statistics of projected low-season flows from these two modeling approaches in July raises confidence in the result. This analysis indicates that the projection of increased high-end flows (the upper 5% or so of the distribution of flows), driven by increased intensity of summer convective rainfall, should be considered a relatively robust hydroclimatic projection.

This study has attempted only rudimentary explanations for why flows at the Gila gage might become systematically lower in June or more variable in July in future decades.

Such diagnostic work will be described in the next phase of this analysis. Ongoing research for the next phase will emphasize the different processes that are important in June and July. In observations we find that June streamflows are poorly correlated with concurrent June precipitation (which is typically very low in this pre-monsoon onset month), and instead are better correlated with the preceding May streamflows. The simulated flow decreases in the BoR simulations are driven by increasing temperatures in these simulations, which are forced by the steady increase in greenhouse gases prescribed by the A1B forcing scenario. Flows in July are much more directly modulated by July precipitation rather than by the preceding month's streamflow.

5. Summary of principal results and conclusions

- The instrumental record of precipitation and streamflow in the upper Gila basin (since 1930) spans more than 80 years. Interannual and decadal variability of precipitation is very large during this period of record, as has been documented in many previous studies. A very significant warming trend occurred during the latter half of the observational period, as documented in recent analyses (e.g. Gutzler and Robbins 2011; Gutzler 2013).
- Observed precipitation in the upper Gila watershed during the low-flow month of June exhibited no significant secular trend in monthly average rainfall in the instrumental record. Most of the distribution of rainfall in June decreased very slightly between the first (1930-1972) and second (1973-2014) halves of the data record. The upper half of the distribution of July monthly precipitation shifted slightly toward higher values, indicating a wetter early monsoon in high-rainfall years, while the lower half of the distribution showed a slight tendency toward lower values. In other words, the overall distribution of precipitation values in July widened between the first and second halves of the record, indicating increased variability of monthly precipitation from year to year at the beginning of the monsoon season.
- Observed streamflow in the upper Gila watershed during the same low-flow months exhibited a modest upward trend in average flow since 1930. The increased flows were manifested as higher values of the upper half of the distribution of monthly flows in both June and July; that is, the average flow increased because high-flow

years were higher in the second half of the data record. June high-flow months increased in the second half of the record, despite a slight decrease in precipitation, because snowmelt runoff increased during this period. Months with below-average streamflow exhibited essentially no trend in the data record, i.e. streamflow in low-flow years did not exhibit much change across the instrumental record. These conclusions apply to distribution statistics derived from either monthly or daily data, suggesting that monthly data provide a reasonable proxy for the distribution of expected daily flows in future projections.

- Trends and variability are extremely difficult to separate in the observed data record. The large variability associated with multi-year drought and pluvial spells makes detection of long-term trends very difficult. The extreme drought at the end of the observed record in recent years has a large effect on calculation of long-term "trends".
- Simulated precipitation from an extensive set of climate models exhibited no statistically significant overall trend in median monthly precipitation rate from the mid-20th Century to the mid-21st Century, spanning observed and near-term future climate. The low end of the distribution of precipitation values exhibited no trend over this period of time. However the upper end of the distribution, especially the highest 5-10% of values, spikes upward significantly as the climate warms up. Climatological mean values of precipitation, which are influenced by these extreme wet months, therefore increase somewhat in future decades in association with warmer temperatures. The absence of a significant trend in simulated precipitation, averaged over many simulations, masks very large differences in trends from one individual model simulation to another.
- Simulated streamflow values in June shift toward lower average flows. This signal is consistent among models, despite the ambiguous trends in corresponding simulated precipitation in the upper Gila basin. The change in streamflow is the result of higher temperatures affecting evaporation rates, consistent with many previous studies. The lowest 75% of simulated July flows change vary little with time, but the high-flow months in future years exhibit higher flows.

- The high-flow tail of of the distribution of simulated monthly streamflow *decreases* dramatically in June, but *increases* in July. The latter increase is associated with an inferred increase in episodic extreme precipitation events in July once the monsoon is initiated. Therefore the magnitude of extreme high-flow events during the monsoon season is expected to increase, but the principal change in the pre-monsoon dry season is a diminution of both average and anomalously high flows.

6. References

Cook, B.I., and R. Seager, 2013: The response of the North American Monsoon to increased greenhouse gas forcing . *Journal of Geophysical Research*, 1690-1699.

Daly, C., Halbleib, M., Smith, J. I., Gibson, W. P., Doggett, M. K., 2008: Physiographically sensitive mapping of climatological temperature and precipitation across the conterminous united states. *International Journal of Climatology* **28**, 2031-2064.

Douglas, M.W., R.A. Maddox and K. Howard, 1993: *The Mexican Monsoon*. *Journal of Climate* **6**, 1665-1677.

Etheredge, D., D.S. Gutzler and F.J. Pazzaglia, 2004: Geomorphic response to seasonal variations in rainfall in the Southwest United States. *GSA Bulletin* **116**, 606-618.

Garfin, G., H.-I. Chang and M. Switanek, 2014: Climate and hydrology of the upper Gila River basin. Chapter 3 in *Gila River Flow Needs Assessment* (Gori et al. 2014, cited below), p. 40-79.

Gori, D., M.S. Cooper, E.S. Soles, M. Stone, R. Morrison, T.F. Turner, D.L. Propst, G. Garfin, M. Switanek, H. Chang, S. Bassett, J. Haney, D. Lyons, M. Horner, C.N. Dahm, J.K. Frey, K. Kindscher, H.A. Walker and M.T. Bogan, 2014: *Gila River Flow Needs Assessment.* A report by The Nature Conservancy, 515 pp. [obtained online August 4, 2014, at http://nmconservation.org/Gila/GilaFlowNeedsAssessment.pdf]

Gutzler, D.S., 2013: Streamflow projections for the upper Gila River. Report submitted to the New Mexico Interstate Stream Commission, 39 pp. Final version dated December 10, 2013. [http://nmawsa.org/ongoing-work/streamflow-projections-for-the-upper-gila-river-considering-climate-change/draft-stream-flow-projections-for-the-upper-gila-river/view]

-----, 2014: Review of "Climate and Hydrology of the Upper Gila River Basin" by G. Garfin, H.-I. Chang and M. Switanek: Chapter 3 of *Gila River Flow Needs Assessment*. Report submitted to the New Mexico Interstate Stream Commission, 15 pp. Final version dated October 10, 2014. [http://nmawsa.org/ongoing-work/nature-conservancys-gila-flow-needs-assessment-chapter-reviews-2014/review-gila-flow-needs-assessment-chapter-3/view]

-----, and J.W. Preston, 1997: Evidence for a relationship between spring snow cover and summer rainfall in New Mexico. *Geophysical Research Letters* **24**, 2207-2210.

-----, and T.O. Robbins, 2011: Climate variability and projected change in the western United States: regional downscaling and drought statistics. *Climate Dynamics,* **37**, 835-849.

-----, and S.J. Keller, 2011: Observed trends in snowpack and Spring season soil moisture. *New Mexico Journal of Science* **46**, 169-182.

Hales, J. E., 1972, Surges of maritime tropical air northward over the Gulf of California. *Monthly Weather Review* **100**, 298-306.

Higgins, R.W., Y. Yao, and X.-L. Wang, 1997: Influence of the North American monsoon system on the U.S. summer precipitation regime. *Journal of Climate* **10**, 2600-2622.

IPCC, 2007: *Climate Change 2007: The Physical Science Basis.* Working Group I Contribution to the Fourth Assessment Report of the Intergovernmenal Panel on Climate Change, Cambridge University Press, 996 pp.

-----, 2013: *Climate Change 2013: The Physical Science Basis.* Working Group I Contribution to the Fifth Assessment Report of the Intergovernmenal Panel on Climate Change, Cambridge University Press, 1535 pp.

Jones, S.M., and D.S. Gutzler, 2016: Spatial and seasonal variations in aridification across southwest North America. *Journal of Climate* **29**, in press.

Horner, M. and C.N. Dahm, 2014: Ecohydrology and Recent Climatology of the Gila River . Chapter 2 in *Gila River Flow Needs Assessment* (Gori et al. 2014, cited above), p. 4-39.

Liang, X., D.P. Lettenmaier, E.F. Wood and S.J. Burges, 1994: A simple hydrologically based model of land surface water and energy fluxes for General Circulation Models. *Journal of Geophysical Research* **99**, 14415–14428.

Meehl G.A., C. Covey, T. Delworth, M. Latif B. McAvaney, J.F.B. Mitchell and R.J. Stouffer, 2007: The WCRP CMIP3 multi-model dataset: A new era in climate change research. *Bulletin of the American Meteorological Society* **88**, 1383-1394.

Pascolini-Campbell, M.A., R. Seager, D.S. Gutzler, B.I. Cook and D. Griffin, 2015: Causes of interannual to decadal variability of Gila River streamflow over the past century. *Journal of Hydrology* **3**, 494-508. [http://www.sciencedirect.com/science/article/pii/S2214581815000178]

Reclamation, 2011a: SECURE Water Act Section 9503(c): Reclamation Climate Change and Water. U.S. Department of the Interior, Bureau of Reclamation Report to Congress, 206 pp.

-----, 2011b: West-Wide Climate Risk Assessments: Bias-Corrected and Spatially Downscaled Surface Water Projections. U.S. Department of the Interior, Bureau of Reclamation, Technical Services Center, Denver CO, 122 pp.

Redmond, K.T., and R.W. Koch, 1991: Surface climate and streamflow variability in the western United States and their relationship to large-scale circulation indices. *Water Resources Research* **27**, 2381-2399.

Ritchie, E.A., K.M. Wood, D.S. Gutzler and S.R. White, 2011: The influence of eastern Pacific tropical cyclone remnants on the southwestern United States. *Monthly Weather Review* **139**, 192-210.

Ropelewski, C. F. and M. S. Halpert, 1986, North American precipitation and temperature patterns associated with the El Niño/Southern Oscillation (ENSO). *Monthly Weather Review* **114**, 2352-2362.

Taylor K.E., R.J. Stouffer and G.A. Meehl, 2012: An overview of CMIP5 and the experiment design. *Bulletin of the American Meteorological Society* **93**, 485–498.

Tuan, Y. F., C. E. Everard, J. G. Widdison, and I. Bennett, 1973: *The climate of New Mexico*, Rev. ed. New Mexico State Planning Office, 197 pp.

Fig 1

Figure 1. Map of the upper Gila basin, adapted from USGS site location metadata (http://waterdata.usgs.gov/nwis/nwismap/?site_no=09430500&agency_cd=USGS). The gray pointer near the bottom of the plot indicates the location of the Gila gage (USGS gage 09430500), which is the principal streamflow analysis point for this study. The gage elevation is 4655 ft ASL, with an upstream contributing drainage area of 1864 mi^2.

Fig 2

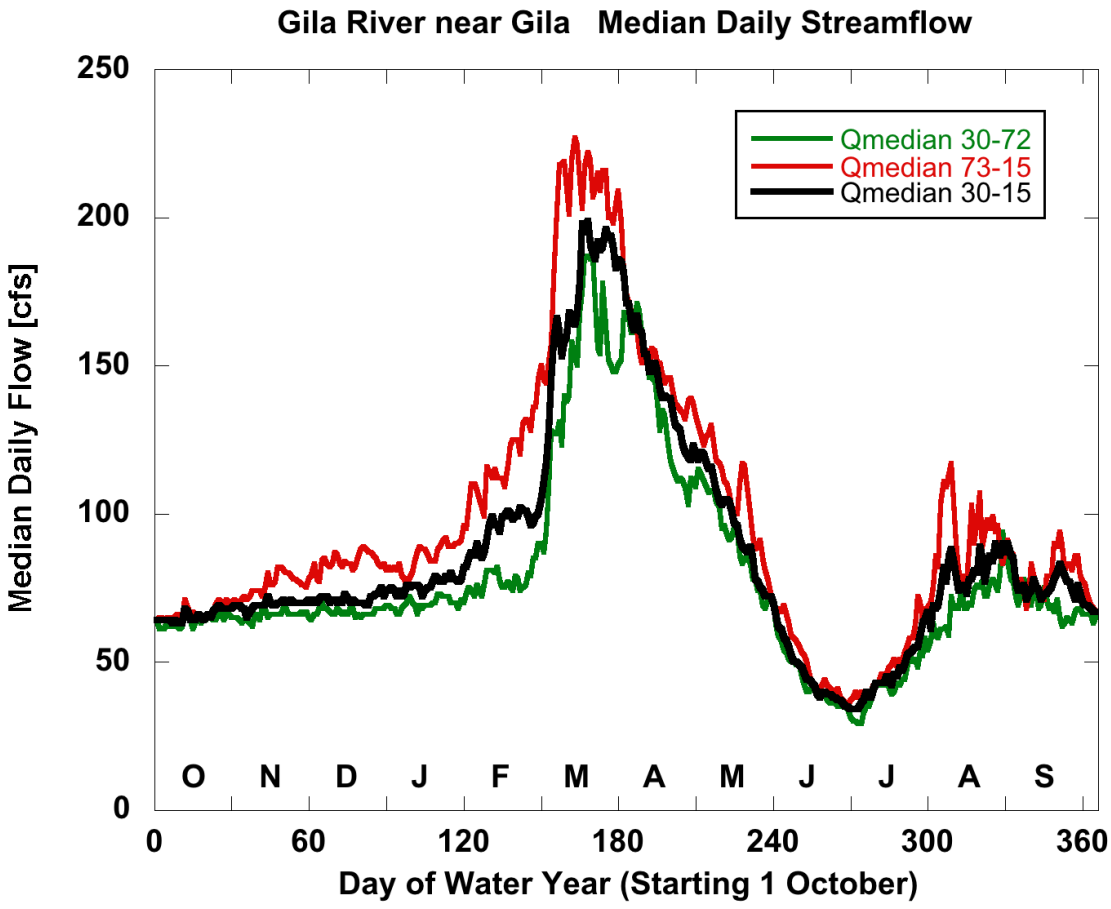

Figure 2. Hydrographs of observed streamflow at the Gila gage on the Gila River (USGS 09430500), similar to the plot introduced by Gutzler (2013) but updated through WY 2015. The thick black line shows the median daily flow for each day of the Water Year (day 1 = Oct 1, day 365 = Sep 30) for the 86-year period Oct 1929 – Sep 2015 (WY 1930-2015). The green line shows the median flow based on just the first half of the period of record (WY 1930-1972). The red line shows the median daily flow based on just the second half of the record (WY 1973-2015). Months of the year are indicated between tick marks on the x-axis.

Fig 3

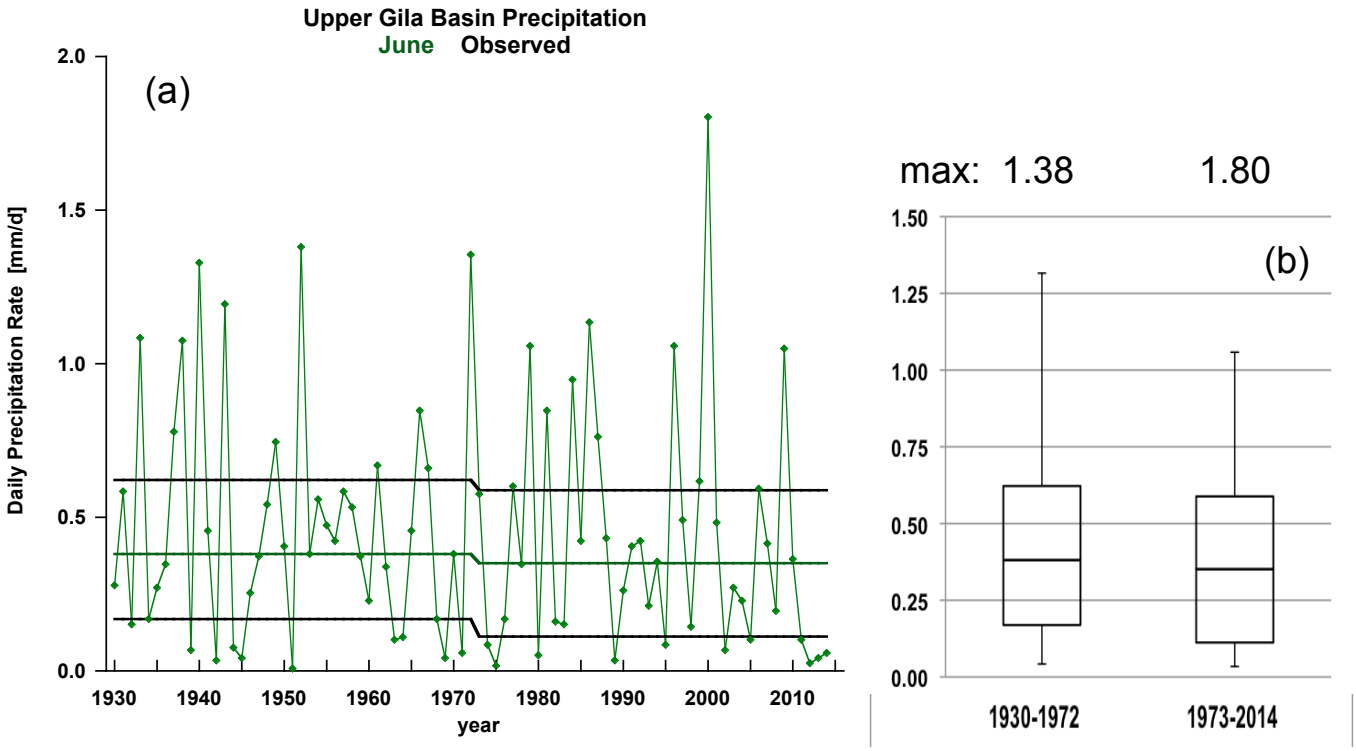

Figure 3. Time series and distribution of **observed June monthly precipitation rate** in the upper Gila River watershed, 1930-2014.

a) Time series of monthly June averages of daily precipitation rate (mm/d). Horizontal lines indicate the values of the 25th, 50th, and 75th percentiles of monthly precipitation, calculated separately for the first half (1930-1972) and second half (1973-2014) of the data record.

b) Box-and-whiskers plots of the distributions of monthly values of June precipitation rate corresponding to the time series in (a). The box is delineated by the 25th and 75th percentiles, and the line in the interior of each box is the median monthly value (the 50th percentile; these percentile values are the same as those shown in the time series in (a). Whiskers denote the 5th and 95th percentile values of monthly mean precipitation rate.

Fig 4

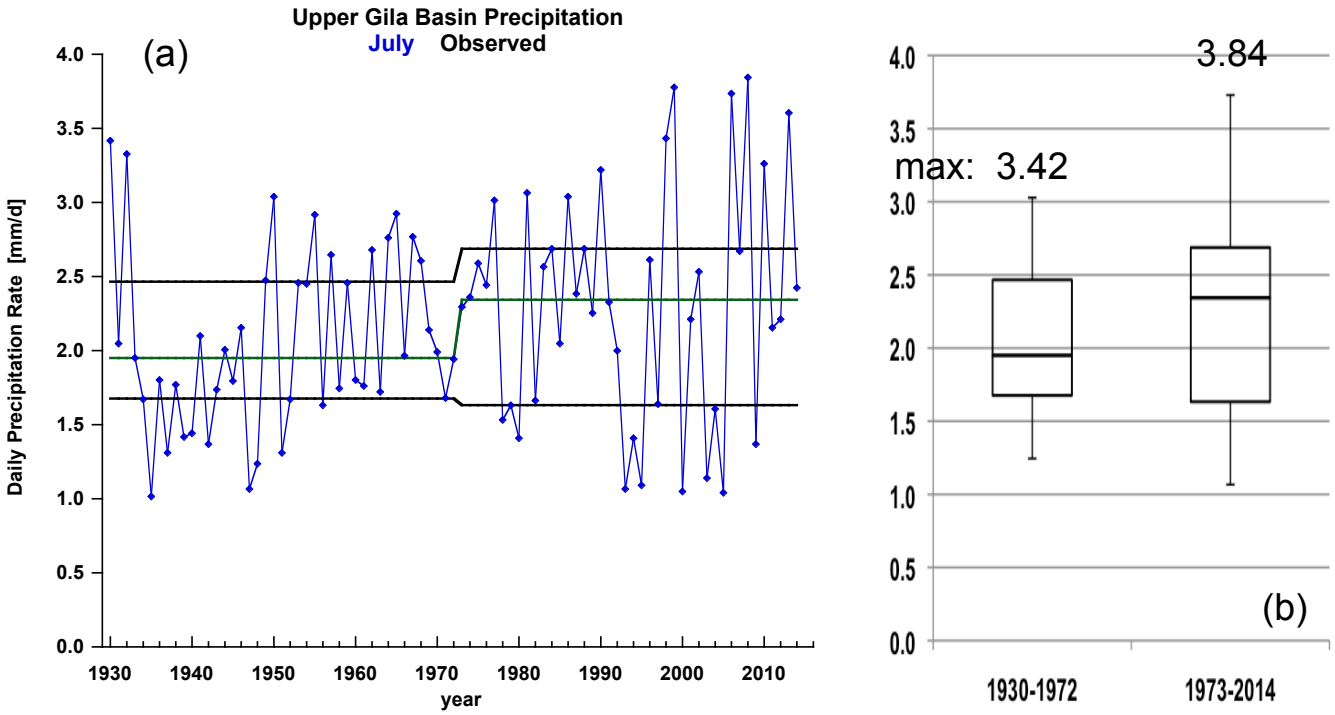

Figure 4. Like Figure 3, but for **observed July precipitation rate** in the upper Gila watershed.

Fig 5

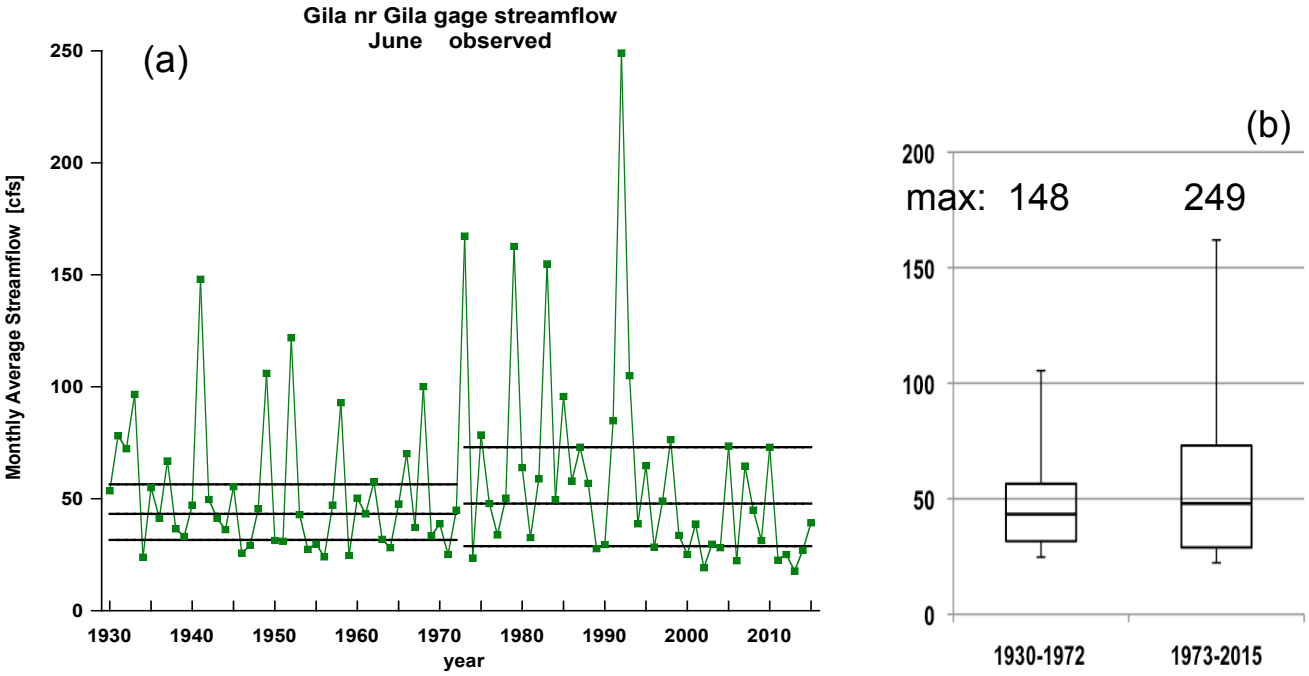

Figure 5. Time series and distribution of **observed June monthly streamflow** at the Gila gage, 1930-2015.

a) Time series of monthly June averages of daily streamflow (cfs). Horizontal lines indicate the values of the 25th, 50th, and 75th percentiles of monthly precipitation, calculated separately for the first half (1930-1972) and second half (1973-2015) of the data record.

b) Box-and-whiskers plots of the distributions of monthly mean values of June streamflow corresponding to the time series in (a), plotted using the same convention as the plots for precipitation in Figs. 3 and 4.

Fig 6

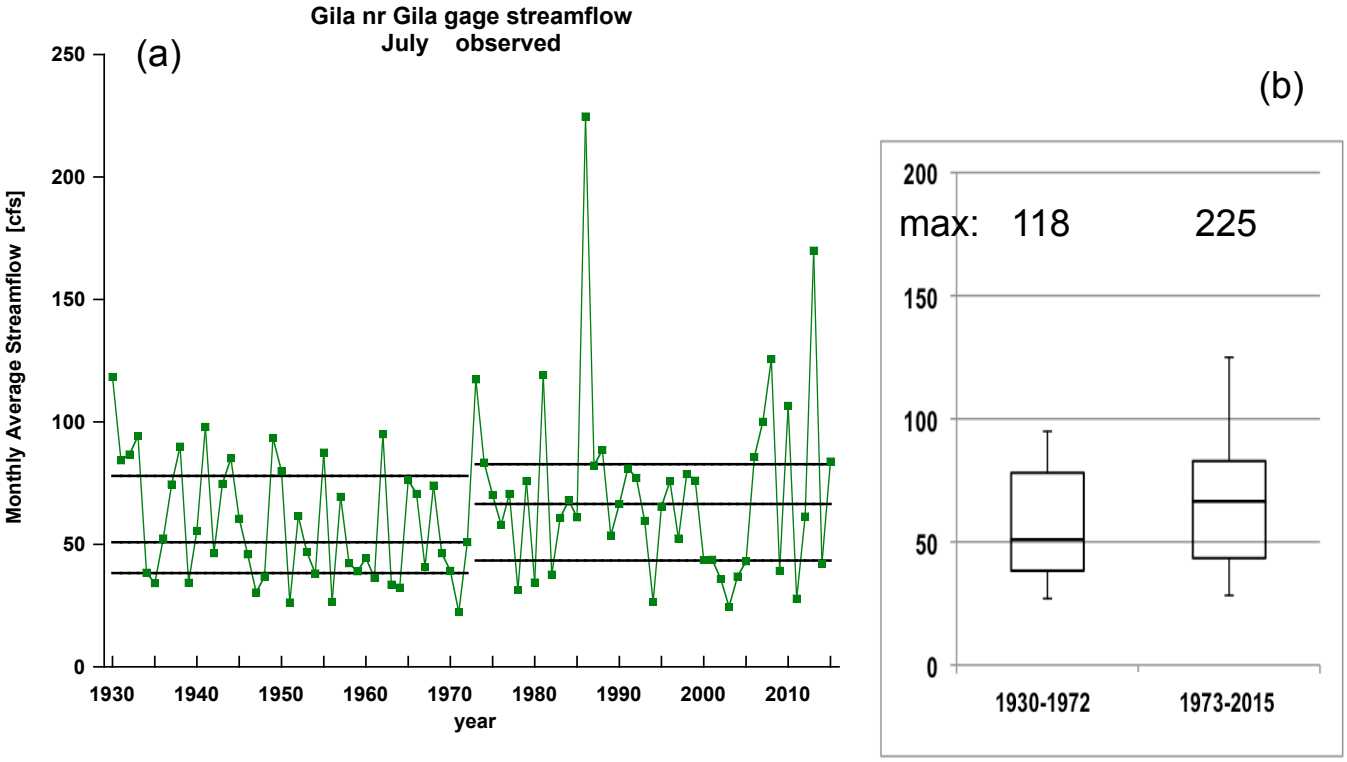

Figure 6. Time series and distribution of **observed July monthly streamflow** at the Gila gage, 1930-2015, analogous to the plots for June streamflow in Fig. 4.

Fig 7

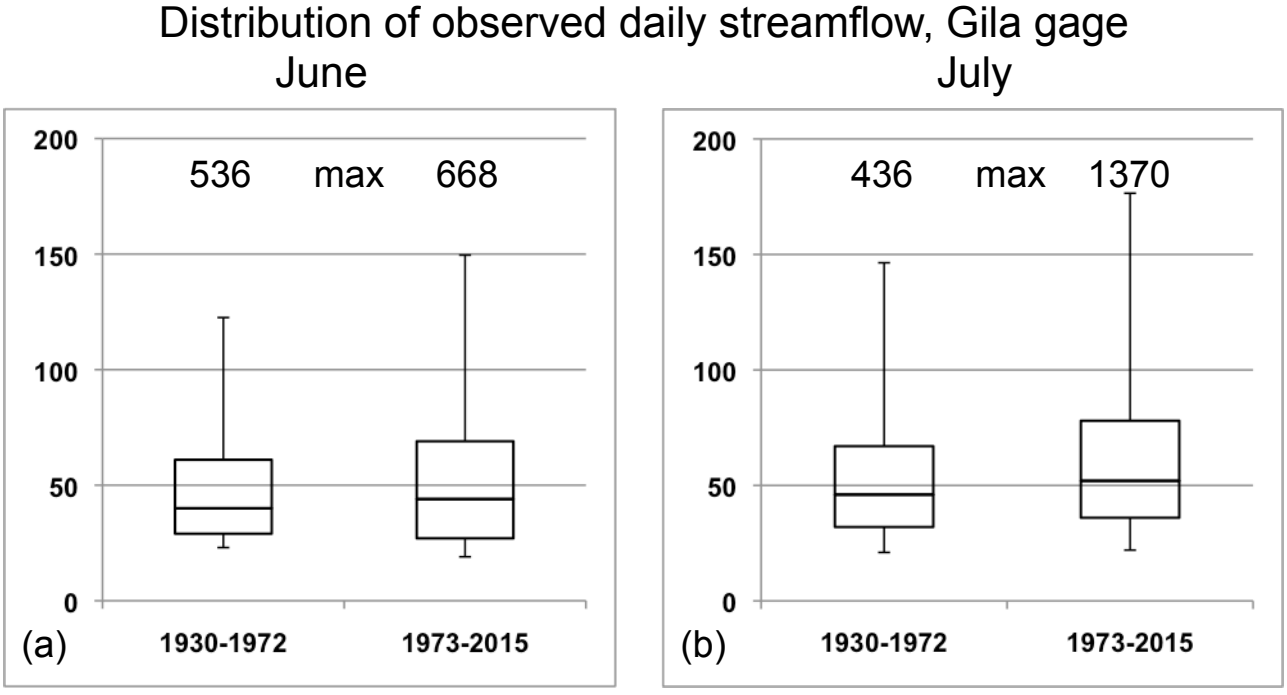

Figure 7. Distribution of **daily observed streamflow in (a) June and (b) July** at the Gila gage, 1930-2015, calculated separately for the first and second halves of the data record (units cfs). The maximum daily flow in each half of the data record is shown above the 95th percentile whisker for each month and half of the record.

Fig 8

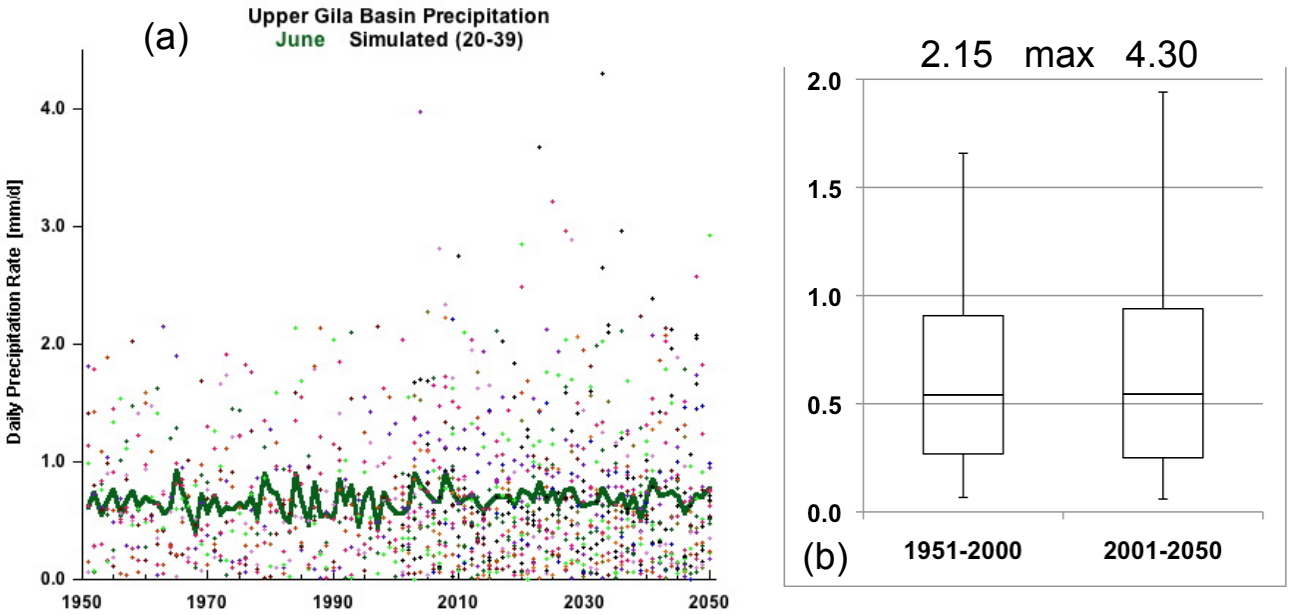

Figure 8. Time series and distribution of **simulated June monthly precipitation rate** (units mm/d), 1951-2050, derived from 39 global climate model simulations downscaled to the upper Gila basin.

a) Time series: Each dot represents June precipitation rate from a single simulation, with 20 of the 39 simulations represented on this plot. (The other 19 simulations are included in the analysis but not shown here to make the figure easier to read.) The heavy solid line denotes the median value of all 39 simulations.

b) Distribution of simulated June monthly precipitation rates, using all 39 simulations, calculated separately over the first half (1951-2000) and second half (2001-2050) of the simulation period. Like the distribution plots for observed precipitation and streamflow (Figs. 3-6), the box denotes 25th, 50th, and 75th percentile values, and the whiskers denote the 5th and 95th percentile values.

Fig 9

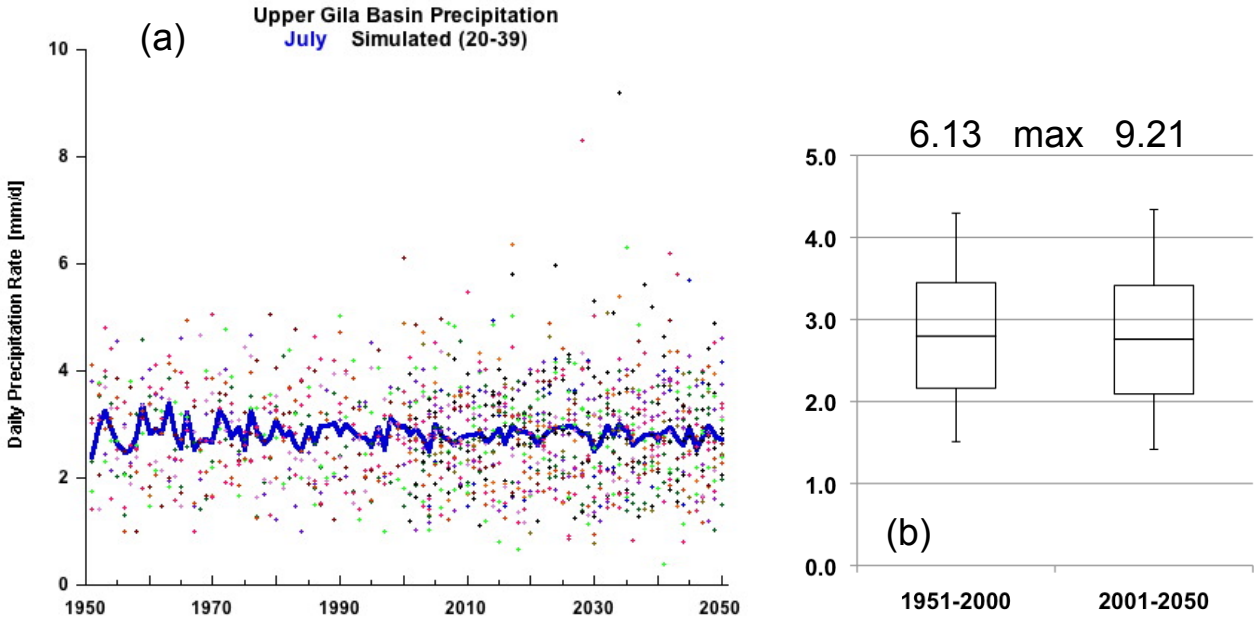

Figure 9. Time series and distribution of **July simulated monthly precipitation rate** (mm/d), 1951-2050, derived from 39 global climate model simulations downscaled to the upper Gila basin, analogous to the June simulated precipitation plots in Fig. 8.

a) Time series of 20 (of 39) July simulated monthly precipitation rates.

b) Distribution of July simulated monthly precipitation rates.

Fig 10

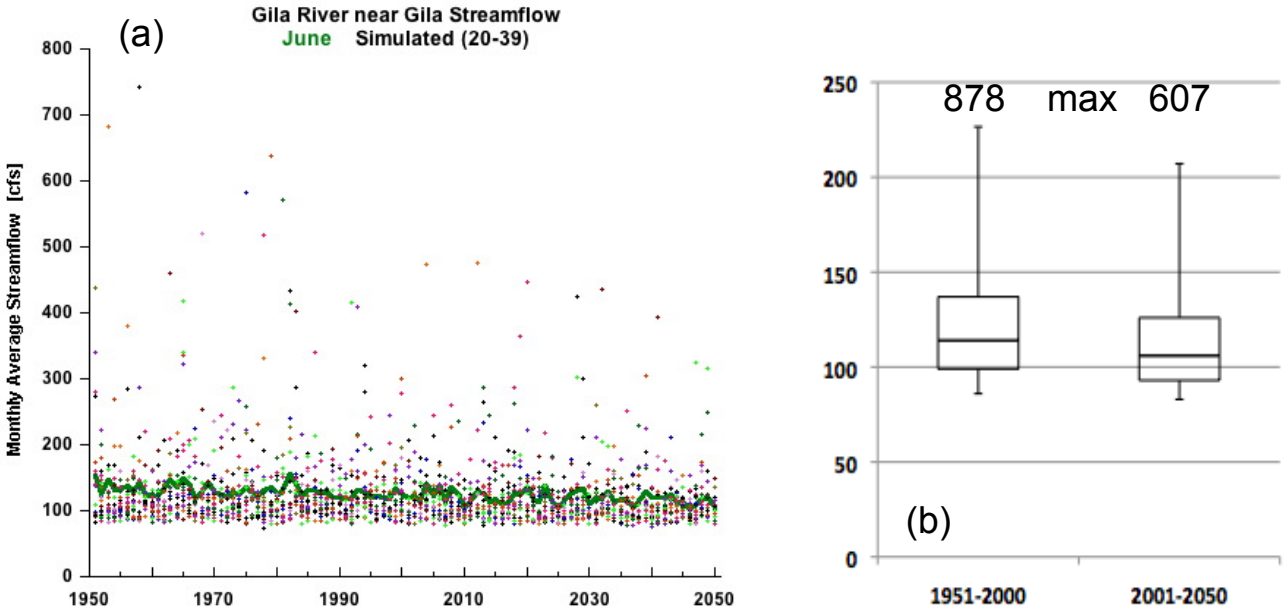

Figure 10. Time series and distribution of **simulated June streamflow** (cfs) at the pour point corresponding to the Gila gage, 1951-2050, derived from 39 global climate model simulations downscaled to the upper Gila basin.

a) Time series of 20 (of 39) simulations, plotted using the same convention as the simulated precipitation plots for June and July in Figs. 8 and 9.

b) Distribution of June monthly flows, plotted using the same convention as the simulated precipitation plots for June and July in Figs. 8 and 9.

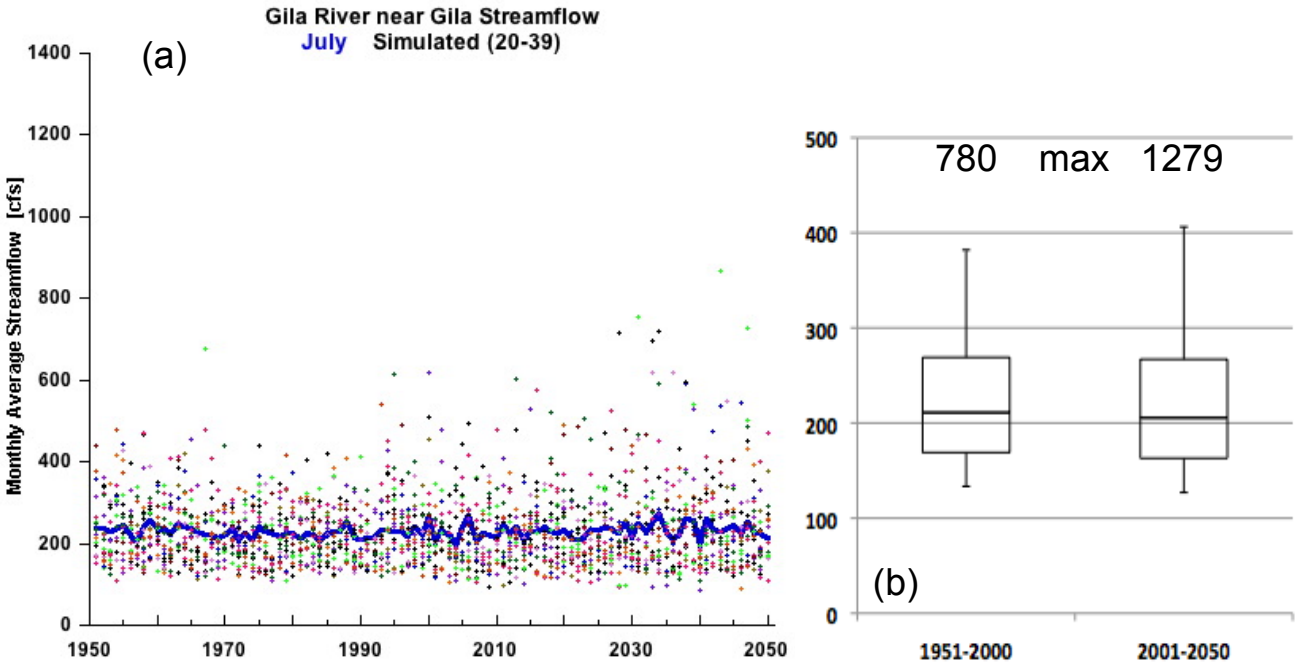

Figure 11. Time series and distribution of **simulated July streamflow** (cfs) at the pour point corresponding to the Gila gage, 1951-2050, derived from 39 global climate model simulations downscaled to the upper Gila basin.

a) Time series of 20 (of 39) simulations, analogous to the simulated June streamflow distribution plot in Fig. 10, plotted using the same convention as the simulated precipitation plots for June and July in Figs. 8 and 9.

b) Distribution of July streamflow values from all 39 simulations, analogous to the simulated June streamflow distribution plot in Fig. 10.